SvedbergOpen
DISSEMINATION OF KNOWLEDGE

International Journal of Artificial Intelligence and Machine Learning

Publisher's Home Page: https://www.svedbergopen.com/

Research Paper Open Access

Strength and Compaction Behaviour of Fly Ash–Stabilised Red Soil Reinforced with Biaxial Geogrids: Experimental Investigation and Artificial Neural Network Modelling

Banushree. T[1], H.C. Muddaraju [2]

[1.]Research Scholar, Department of Civil Engineering, UVCE, Bangalore University, Bangalore 560056, Karnataka, India.
E-mail: banushreegowda15@gmail.com
[2.]Associate Professor, Department of Civil Engineering, UVCE, Bangalore University, Bangalore 560056, Karnataka, India.
E-mail: muddarajuhc@uvce.ac.in

Abstract
This study evaluates the combined effect of Class F fly ash stabilisation and biaxial geogrid reinforcement on the compaction and strength behaviour of red soil intended for use as a flexible pavement subgrade, and develops an artificial neural network (ANN) model of the reinforced system. Red soil obtained from the Bangalore University campus, Jnanabharathi, was blended with fly ash at dosages from 2% to 60% by dry weight for compaction testing and from 2% to 20% for strength testing, and assessed through Standard Proctor, California Bearing Ratio (CBR) and Unconfined Compressive Strength (UCS) tests. A fly ash content of 10% gave the highest maximum dry density, UCS and CBR and was adopted as the optimum dosage; it raised the soaked CBR at 2.5 mm penetration from 1.40% to 9.31% and the unsoaked CBR from 4.66% to 14.43%. Three biaxial polypropylene geogrids of differing tensile strength and aperture size — 40 kN/m (38 mm aperture), 20 kN/m (38 mm aperture) and 4.07 kN/m (8 mm aperture) — were introduced into the optimally stabilised soil as single layers at H/2, H/3 and H/4 and as a double layer at H/4 from both faces, where H is the specimen height. Because the aperture of two geogrids exceeded the diameter of the conventional 38 mm UCS specimen, a large-scale mould of 100 mm internal diameter was fabricated so that representative soil–geogrid interlock could develop. Reinforcement at H/4 was the most effective single-layer position for all three geogrids, and double-layer reinforcement produced the largest gain, raising the UCS of the stabilised soil from 300 kPa to 565 kPa. The 4.07 kN/m geogrid outperformed the two higher-strength products at every position. A feed-forward ANN with two hidden layers, trained on the thirteen large-scale UCS configurations and validated by nested leave-one-out cross-validation, predicted UCS with R^2 = 0.969 and RMSE = 16.4 kPa against R^2 = 0.671 and RMSE = 53.3 kPa for multiple linear regression, confirming that the reinforced response is strongly non-linear. Sensitivity analysis of the trained network ranked the number of reinforcement layers as the dominant variable and, among the geogrid product properties, placed aperture size above tensile strength. A second network used as a continuous surrogate over the fly ash dosage range located the CBR optimum at approximately 9% fly ash. The results support the combined use of a low fly ash dosage and a small-aperture biaxial geogrid for improving weak red soil subgrades, and indicate that specifications written around geogrid tensile strength alone may select a less effective product.

Keywords: Red soil; Class F fly ash; biaxial geogrid; subgrade stabilisation; aperture size; artificial neural network; California Bearing Ratio (CBR); Unconfined Compressive Strength (UCS)

1.Introduction

The performance and service life of a flexible pavement are governed to a large extent by the engineering behaviour of the supporting subgrade. Weak subgrade soils generally exhibit low bearing capacity, high compressibility and excessive deformation under repeated traffic loading, which manifests at the surface as rutting, differential settlement and premature fatigue cracking. Improving the mechanical response of such soils is therefore central to the construction of durable and economical pavement systems, particularly in regions where the naturally occurring subgrade is a fine-grained residual soil.

Two broad strategies are available for this purpose. The first is chemical or mechanical stabilisation of the soil itself, most commonly by blending it with an industrial by-product such as fly ash. The second is the inclusion of planar geosynthetic reinforcement, which mobilises tensile resistance and lateral confinement within the soil mass. Both approaches are well established individually; their combined use, and in particular the influence of geogrid geometry rather than geogrid tensile strength, has received considerably less attention. The present study addresses that gap for red soil, a residual lateritic soil that is widely distributed across peninsular India and is routinely encountered as subgrade material in the Bangalore region.

1.1 Review of related studies

Fly ash utilisation in geotechnical works has been driven both by performance and by the need to divert a bulk waste stream from ash ponds and landfills [13]. Gyanen et al. [5] reported that blending fly ash with fine-grained soil altered the compaction characteristics, reducing the maximum dry density at high replacement levels while improving strength up to a limiting dosage. Ozdemir [12] observed a marked increase in the bearing capacity of a soft soil following fly ash addition, and attributed the improvement to densification and to the modified grain-size distribution of the blend. Partab Rai and Qiu [14] examined fly ash together with cement and showed that the strength gain of the blended subgrade depends strongly on the availability of calcium for cementitious reaction. Baskar et al. [3] combined fly ash with calcium carbide residue and demonstrated that an external source of lime is required before appreciable pozzolanic strength development occurs in a Class F ash. A consistent finding across these studies is the existence of an optimum fly ash content beyond which strength declines, although the reported optimum varies widely with the parent soil and with the class of ash used.

Geosynthetic reinforcement of subgrades and unpaved layers has a similarly long record. Giroud and Noiray [8] provided one of the earliest design treatments of geotextile-reinforced unpaved roads, framing the benefit in terms of improved stress distribution and reduced rut depth. Fannin and Sigurdsson [7] confirmed these benefits under field conditions. Kamel et al. [9] showed experimentally that geogrid inclusion in a subgrade soil increases CBR and reduces deformation through interlocking and interface friction, and that the depth of placement is a controlling variable. Choudhary et al. [4] reported CBR improvement in expansive subgrades using a single reinforcement layer, while Duncan-Williams and Attoh-Okine [6] examined the influence of geogrid on granular base strength. Singh et al. [11] and Rajesh et al. [15] both studied the engineering performance of geogrid-reinforced soft subgrades and identified an optimum reinforcement depth expressed as a fraction of the layer thickness. Deshmukh et al. [16] extended the evidence to field scale by measuring the improvement in composite modulus of geosynthetic-reinforced pavements, and Calvarano and Palamara [10] reviewed reinforcement of unpaved roads. Abd El Halim et al. [2] and AASHTO [1] address the analogous reinforcement of bound layers and the standardisation of geosynthetic base reinforcement respectively.

Studies that combine the two techniques are fewer. Jayawardane and Anggraini [17] investigated geotextile-reinforced fly ash-based geopolymer stabilised residual soil and reported that the reinforcement and the stabiliser act on different mechanisms and are broadly additive. However, the majority of laboratory investigations of soil–geogrid interaction employ the conventional 38 mm diameter UCS specimen. Where the geogrid aperture is of the same order as, or larger than, the specimen diameter, the reinforcement cannot develop representative interlock and the measured contribution is dominated by boundary effects. This limitation is rarely acknowledged and is a plausible reason for the scatter reported in the literature regarding the influence of geogrid tensile strength.

1.2 Research significance and objectives

Against this background, the present investigation was designed to answer three questions. First, what is the optimum Class F fly ash dosage for the red soil considered, judged simultaneously on compaction, UCS and CBR response? Second, at what depth, and in how many layers, should biaxial geogrid be placed within the stabilised soil to maximise strength gain? Third, and most importantly, does the tensile strength of the geogrid or its aperture geometry exert the dominant influence on reinforcement efficiency in a fine-grained stabilised subgrade? To answer the third question meaningfully, a large-scale UCS mould of 100 mm internal diameter was fabricated so that geogrids with apertures of 38 mm could be tested without the boundary constraint imposed by the standard mould. The outcome is intended to inform the selection of geogrid products for subgrade improvement, where specification is commonly written around tensile strength alone.

1.3 Artificial neural networks in geotechnical modelling

Laboratory programmes of the kind described above generate a modest number of observations across several interacting variables, and the relationships between those variables are rarely linear. Artificial neural networks have therefore been applied widely in geotechnical engineering to relate mixture and reinforcement parameters to measured strength, and comprehensive reviews of the approach and of its pitfalls in this field are available [22, 23]. Applications directly relevant to the present work include the prediction of the CBR and unconfined compressive strength of stabilised subgrade soils from mixture proportions [24, 25]. The recurring methodological weakness in this literature is validation: models are frequently reported on the basis of a training-set correlation coefficient, or on a single arbitrary train–test split, neither of which provides an unbiased estimate of predictive accuracy when the dataset is small. Shahin et al. [23] identify this explicitly as a limitation of much published work. In the present study the network is therefore validated by nested leave-one-out cross-validation, in which the architecture and regularisation parameter are selected inside an inner resampling loop so that no information from the held-out observation influences either model selection or model fitting, and its performance is benchmarked against a multiple linear regression trained and validated identically.

2.Materials Used

The red soil used in this work was obtained from the Bangalore University campus, Jnanabharathi, Bangalore. Class F fly ash conforming to ASTM C618-03 [18], collected from the Raichur Thermal Power

Station, Karnataka, was used as the stabilising admixture. The sum of SiO_2 + Al_2O_3 + Fe_2O_3 for the ash exceeds 70%, which satisfies the ASTM C618 requirement for a Class F pozzolan. It should be noted that a Class F ash is pozzolanic but not self-cementing: its free lime content is low, so in the absence of an added calcium source such as lime or cement the pozzolanic reaction proceeds slowly and contributes little to short-term strength. The improvements reported in this study, all of which were measured on specimens tested immediately after compaction or after a four-day soak, should therefore be understood as arising predominantly from mechanical stabilisation — improved gradation, void filling and denser particle packing — rather than from cementitious bonding. The physical properties of the red soil and the fly ash are summarised in Table 1.

Table.1: Physical Characteristics of Flyash and Red soil.

Description	**Flyash**	**Red soil**
Colour	Grey	Red
Specific gravity	2.02	2.65
Liquid limit (%)	25.26	37
Plastic limit (%)	nonplastic	21
Free swell index (%)	No swell seen	No swell seen
Shrinkage limit (%)	--	14
Sand size fraction (%)	17.4	53.6
Silt and clay size fraction (%)	82.6	46.4
OMC (%)	18.11	16.5
MDD (g/cc)	1.37	1.78
UCS (kPa)	59.5	344

Reinforcement: Three types of biaxial polypropylene geogrids with different tensile strength 40kN/m (G1), 20kN/m (G2) and 4.07kN/m(G3) are selected as the geogrids reinforcement in this study as shown in the Fig.1 and comparison is done according to its specifications, strength and durability. The geogrid properties as provided by the manufacturer (M/s. Geotech Industries Pvt Ltd, Gujarat) are given in Table 2.

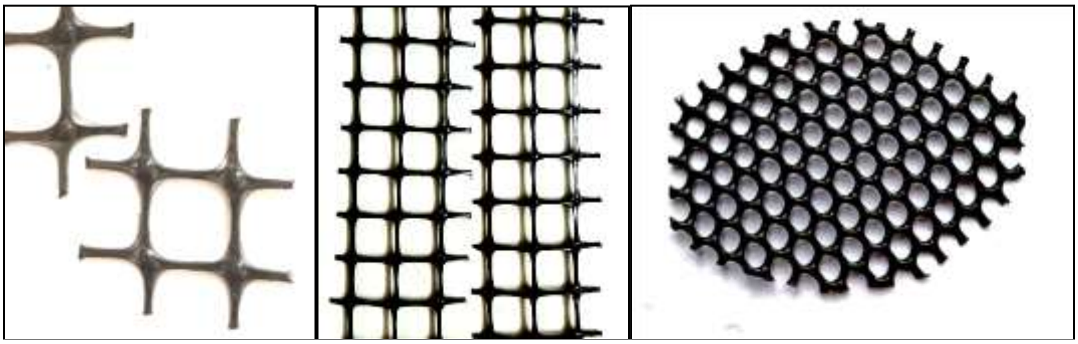

(a) G1 (T= 40kN/m) (b) G2 (T= 20kN/m) (c) G3 (T= 4.07kN/m)

Fig .1: Biaxial Polypropylene Geogrids

Table 2*:* Properties of Biaxial Geogrids

Geogrid Type	**G1**	**G2**	**G3**
Structure	Biaxial, Square Aperture	Biaxial, Square Aperture	Biaxial, Oval Aperture
Polymer	Polypropylene		
Aperture Size (mm)	38	38	8
Tensile Strength (kN/m)	40	20	4.07

3. SAMPLE PREPARATION

The experimental program was conducted to determine the optimum fly ash content for stabilizing red soil and to evaluate the influence of biaxial geogrid reinforcement on its mechanical behavior. The compaction characteristics of the natural soil were first determined using the Standard Proctor test in accordance with IS 2720 (Part 7), from which the optimum moisture content (OMC) and maximum dry density (MDD) were obtained. These parameters were adopted for preparing all specimens.Red soil was blended with different percentages of Class F fly ash by dry weight, and the strength characteristics of each mixture were evaluated using California Bearing Ratio (CBR) and Unconfined Compressive Strength (UCS) tests following the relevant provisions of IS 2720. Based on the experimental results, 10% fly ash was identified as the optimum stabilizer content and selected for the reinforcement study.

For the CBR tests, the required mass of the soil–fly ash mixture was calculated using the corresponding MDD, and water equal to the OMC was added to obtain uniform moisture distribution. The mixture was compacted in layers inside the CBR mould. Circular biaxial geogrid discs, trimmed slightly smaller than the mould diameter, were inserted at predetermined locations during compaction. Single-layer reinforcement was placed at H/2, H/3, and H/4 from the specimen surface, whereas double-layer reinforcement was provided at H/4 from both the top and bottom surfaces of the specimen, where *H* denotes the specimen height. Both soaked and unsoaked CBR tests were conducted on reinforced and unreinforced specimens, and the corresponding load–penetration responses were recorded. The reinforcement configurations adopted in the CBR specimens are illustrated in **Fig. 2**.

Fig .2: Placing of geogrid at predetermined depth.

To further investigate the effect of reinforcement under compressive loading, UCS tests were performed using a specially fabricated large-scale mould with an internal diameter of 100 mm. The larger specimen size was adopted to minimize boundary effects and provide a more representative evaluation of the soil–geogrid interaction than that obtained using the conventional UCS mould. Geogrid discs were cut to match the mould dimensions and embedded within the specimens during compaction. The reinforcement layouts consisted of single-layer placements at H/2, H/3, and H/4, together with a double-layer arrangement located at H/4 from the top and bottom of the specimen, as shown in **Figs. 3 and 4**. All reinforced and unreinforced specimens were prepared at the corresponding OMC and MDD to ensure consistency throughout the experimental program.

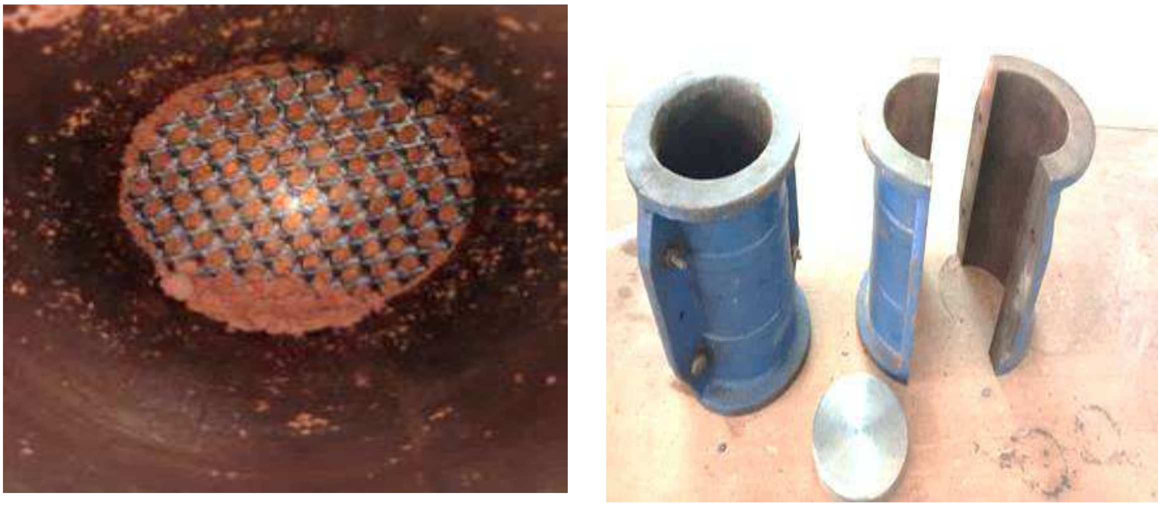

Fig 3: Placement of geogrid in UCS mould during sample preparation

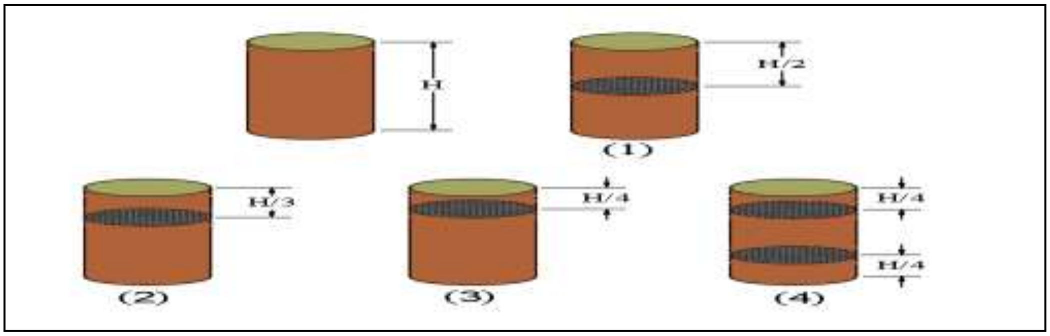

Fig 4: Different combinations of geogrid placement.

4.Results And Discussions

The engineering behavior of red soil stabilized with Class F fly ash was investigated through a comprehensive laboratory testing program. Fly ash was incorporated into the soil at replacement levels of 2%, 4%, 6%, 8%, 10%, 15%, 20%, 30%, 40%, 50%, and 60% (by dry weight of soil) to identify the optimum stabilization content. The stabilized mixtures were evaluated using compaction, Unconfined Compressive Strength (UCS), and California Bearing Ratio (CBR) tests. Based on the optimum fly ash content, the stabilized soil was subsequently reinforced with biaxial geogrids of different tensile strengths, and the effects of reinforcement configuration on the UCS and CBR responses were examined.

4.1 Compaction Characteristics

The influence of fly ash on the compaction behavior of red soil was evaluated using the Standard Proctor test in accordance with IS 2720 (Part 7). Fig 5 presents the variation in optimum moisture content (OMC) and maximum dry density (MDD) with increasing fly ash content.The results indicate that fly ash substantially altered the compaction characteristics of the red soil. The OMC exhibited only minor variations up to a fly ash content of 10%, followed by a gradual decrease at higher replacement levels. This trend may be attributed to the relatively lower water absorption capacity of Class F fly ash compared with the fine-grained soil particles, resulting in a reduced moisture requirement during compaction.
In contrast, the MDD increased progressively with fly ash addition up to 10%, indicating improved packing of the soil matrix. The finer fly ash particles occupied the voids between soil grains, producing a denser particle arrangement and enhancing compaction efficiency. Beyond 10% fly ash, no further improvement in MDD was observed, suggesting that excessive fly ash replaced the soil skeleton without contributing to additional densification. As the fly ash used in this study was predominantly non-pozzolanic, the observed changes in compaction characteristics are primarily attributed to mechanical stabilization rather than cementitious reactions. Based on the combined OMC and MDD responses, the mixture containing **10% Class F flyash** exhibited the most favorable compaction characteristics and was therefore selected as the optimum stabilization level for subsequent UCS and CBR investigations.

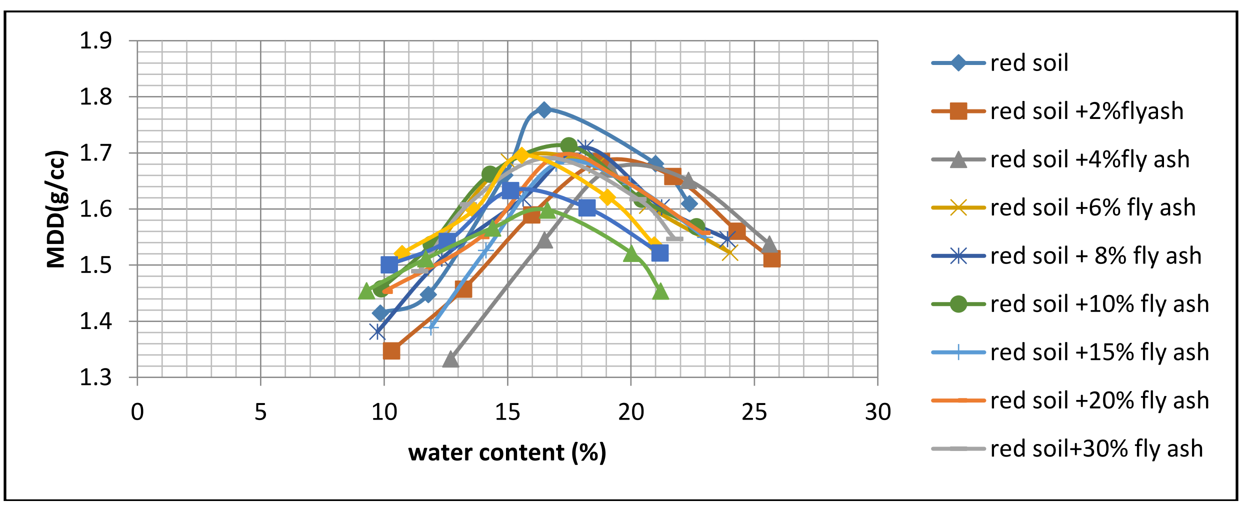

Fig 5: Compaction curves of all combinations of red soil and flyash

4.2 Effect of Unconfined compressive strength (UCS) test and California Bearing Ratio (CBR) Test:
Unconfined Compressive Strength (UCS) Test:

The unconfined compressive strength (UCS) test was conducted to assess the influence of fly ash on the strength characteristics of red soil. The experimental procedure was carried out in accordance with IS 2720 (Part 10): 1991 under controlled laboratory conditions. Test specimens corresponding to each fly ash dosage were prepared at their respective optimum moisture contents (OMC) and compacted to achieve the maximum dry density (MDD). To improve the reliability and repeatability of the experimental observations, three identical specimens were tested for each mixture, and the average value was considered for subsequent analysis. The resulting stress–strain responses are illustrated in Fig. 6.

The experimental results reveal a significant improvement in the compressive strength of red soil following the incorporation of fly ash. The UCS values increased progressively with increasing fly ash content up to an optimum dosage of **10%**, beyond which a gradual decline in strength was observed. Among all the mixtures investigated, the specimen containing **10% flyash** exhibited the highest unconfined compressive strength, demonstrating the most effective stabilization performance.

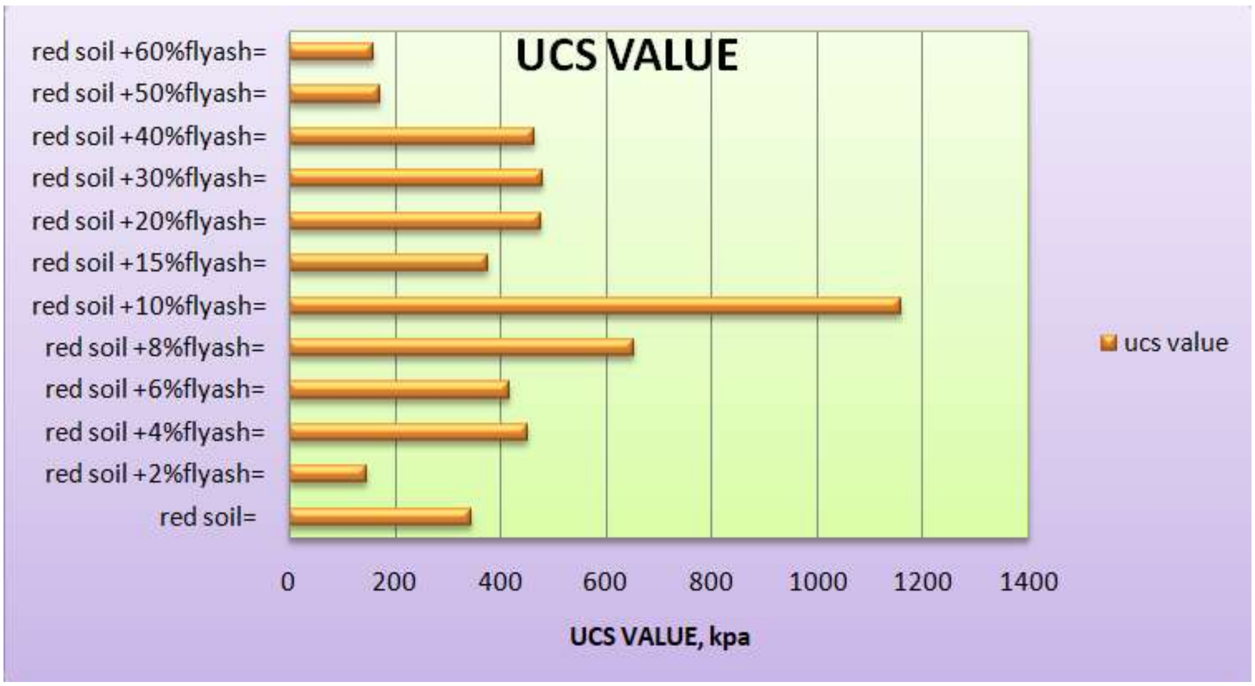

Fig:6: UCS readings of red soil with different percentage of flyash.

The enhancement in strength at lower fly ash contents is primarily associated with improved particle packing and stronger inter-particle bonding between the soil and fly ash particles. The finer fly ash particles occupy the void spaces within the soil matrix, resulting in a denser structure and enhanced resistance to compressive loading. Furthermore, the non-pozzolanic activity of fly ash contributes for strengthening the soil skeleton and improve its mechanical behavior. However, when the fly ash content exceeded the optimum level, the UCS values decreased. This reduction may be attributed to the excessive presence of fly ash particles, which can disrupt the continuity of the soil matrix and promote particle agglomeration. Such agglomeration weakens particle interlocking and reduces the effectiveness of load transfer within the stabilized material. Consequently, the overall compressive strength declines beyond the optimum fly ash dosage.

A comparison with untreated red soil clearly demonstrates that stabilization with **10% flyash** considerably enhances the load-bearing capacity of the soil. Therefore, the results indicate that **10% flyash** represents the optimum stabilization content for maximizing the unconfined compressive strength of the red soil considered in this investigation.

California Bearing Ratio (CBR) Test

The California Bearing Ratio (CBR) test was performed to evaluate the improvement in bearing capacity of fly ash-stabilized red soil for pavement subgrade applications. The tests were conducted in accordance with **IS 2720 (Part 16)**. Specimens were compacted in standard CBR moulds at their corresponding maximum dry densities using heavy compaction energy. Both soaked and unsoaked CBR tests were carried out. For the soaked condition, the compacted specimens were immersed in water for four days before testing, whereas the unsoaked specimens were tested immediately after compaction. The penetration test was conducted at a constant loading rate of **1.25 mm/min**.The experimental CBR values obtained for untreated and stabilized soil mixtures are presented in **Table 3**.

Table 3. Soaked and unsoaked CBR values of fly ash-stabilized red soil.

CBR TEST	(soaked) 2.5mm penetration	(soaked) 5mm penetration	(unsoaked) 2.5mm penetration	(unsoaked) 5mm penetration
red soil	1.40	1.2	4.66	4.1
red soil +2% flyash	2.79	2.4	3.26	3.1
red soil +4% flyash	3.26	2.7	3.73	3.5
red soil +6% flyash	7.45	6.5	8.38	8.07
red soil +8% flyash	8.85	7.1	9.31	7.76
red soil +10% flyash	9.31	7.4	14.43	16.14
red soil +15% flyash	4.66	4.0	6.52	5.59
red soil +20% flyash	5.59	5.2	6.52	6.36

The untreated red soil exhibited low bearing capacity, with soaked and unsoaked CBR values at 2.5 mm penetration of 1.40% and 4.66% respectively. Fly ash addition improved the soaked CBR monotonically up to a dosage of 10%, beyond which the values declined. Under the unsoaked condition the trend was not monotonic: at 2% and 4% fly ash the CBR fell below that of the untreated soil (3.26% and 3.73% against 4.66%) before rising steeply from 6% onwards. This initial reduction is consistent with the ash acting, at low dosages, as a non-plastic filler that interrupts the existing soil fabric without yet forming a continuous denser skeleton; the effect is masked under soaked conditions because the untreated soil itself loses most of its strength on saturation. The maximum soaked and unsoaked CBR values of 9.31% and 14.43% respectively were obtained at 10% fly ash, representing a 6.7-fold and 3.1-fold increase over the untreated soil. This dosage is therefore adopted as the optimum for the reinforcement study.

Two aspects of the CBR results require comment. First, for the mixture containing 10% fly ash the unsoaked CBR at 5.0 mm penetration (16.14%) exceeded that at 2.5 mm (14.43%). IS 2720 (Part 16) provides that where the value at 5.0 mm exceeds that at 2.5 mm the test shall be repeated, and that if the same result is obtained on repetition the higher value shall be adopted as the CBR. The test was repeated and the behaviour was reproduced; the 5.0 mm value is accordingly the governing unsoaked CBR for that mixture. For consistency of comparison across all mixtures, the 2.5 mm values are used throughout the tables and improvement factors reported in this paper, which is the conservative choice. Second, fly ash dosages up to 60% were included in the compaction programme in order to define the full density–dosage relationship, whereas the CBR and UCS programmes were limited to dosages up to 20%. This restriction was adopted because both strength measures had passed their maxima and were falling steadily by 15% to 20% fly ash, so that higher dosages held no prospect of improved strength and lay outside any practical range of application.

The improvement in CBR is attributable to the modified gradation of the blend and to the resulting increase in dry density. The fine ash particles occupy voids between the soil grains, producing a denser and more stable packing and increasing the resistance to penetration. In addition, the addition of the non-plastic ash reduces the plasticity of the matrix and shifts the fabric from a dispersed towards a more flocculated and aggregated arrangement, which contributes to greater stiffness. Beyond the optimum dosage, the CBR declines because the surplus ash progressively replaces load-bearing soil contacts with weaker ash–ash contacts, reducing the structural integrity of the compacted matrix. The magnitude of the improvement — a soaked CBR rising from a value at which the soil would be classified as unsuitable subgrade to one comparable with a moderately competent subgrade — confirms that fly ash stabilisation is an effective and economically attractive treatment for the red soil considered, while simultaneously providing a beneficial outlet for a bulk industrial by-product.

4.3 Influence of Geogrid Reinforcement on CBR Characteristics

Figures 7.1(a), 7.1(b), 7.2(a), 7.2(b), 7.3(a) and 7.3(b) present the soaked and unsoaked California Bearing Ratio responses of fly ash-stabilised red soil reinforced with single and double geogrid layers of differing tensile strength. Geogrid reinforcement improved the bearing capacity of the stabilised soil in every configuration tested, with the magnitude of the improvement depending on both the geogrid used and its depth of placement. The unreinforced stabilised mixture (red soil + 10% fly ash) gave soaked CBR values of 9.31% and 7.40% at 2.5 mm and 5.0 mm penetration and unsoaked values of 14.43% and 16.14% respectively. Introducing the 40 kN/m geogrid (G1) at H/4 raised the soaked values to 12.11% and 10.86% and the unsoaked values to 19.09% and 18.63%. The 20 kN/m geogrid (G2) at the same depth gave soaked values of 11.64% and 10.64% and unsoaked values of 18.16% and 18.00%. The 4.07 kN/m geogrid (G3) at H/4 produced the highest response of the three, with soaked values of 12.18% and 10.55% and unsoaked values of 20.95% and 18.63%. These H/4 results are collated with the corresponding improvement factors in Table 6. Specimens reinforced with two geogrid layers placed symmetrically at H/4 from the top and bottom of the mould followed the same ordering and gave further increases in penetration resistance relative to the single-layer arrangements. Across all three geogrids, H/4 was the most effective single-layer position, and the ranking G3 > G1 > G2 was preserved under both soaked and unsoaked conditions.

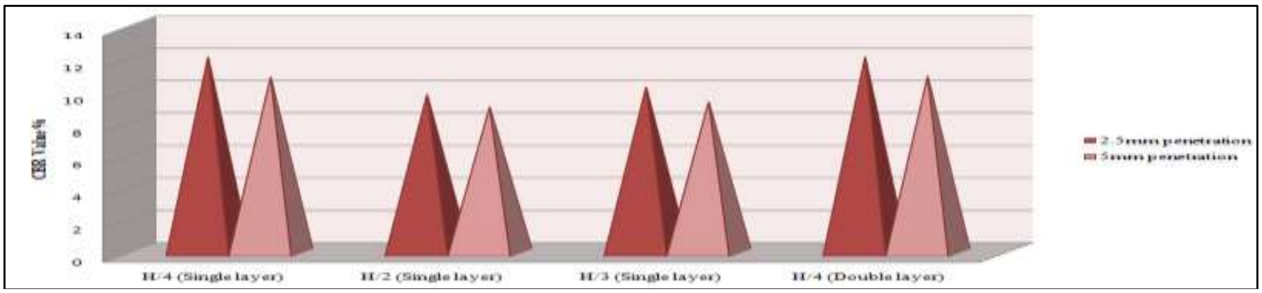

Fig:7.1(a): CBR values with varying position of geogrid reinforcement (40 kN/m tensile strength) for Soaked condition.

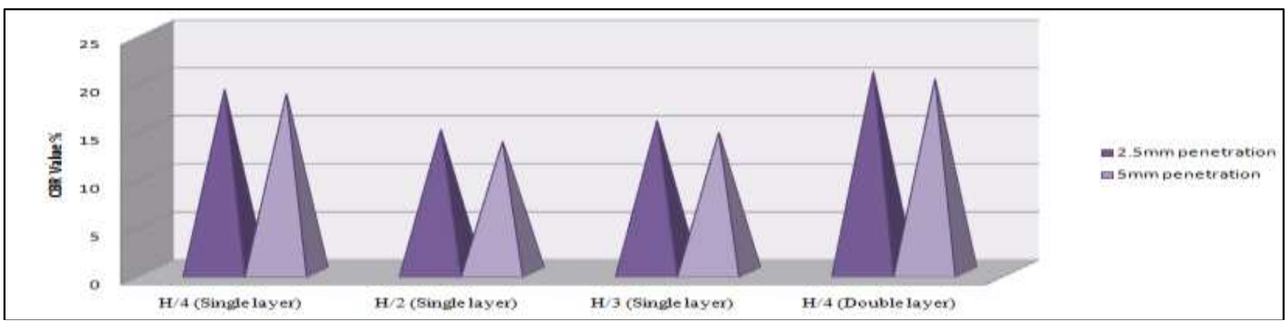

Fig:7.1(b): CBR values with varying position of geogrid reinforcement (40 kN/m tensile strength) for unsoaked condition.

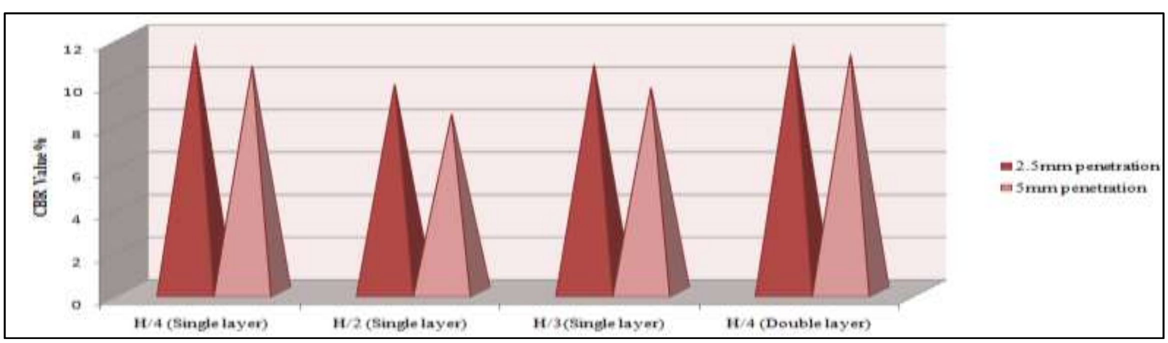

Fig :7.2(a): CBR values with varying position of geogrid reinforcement (20 kN/m tensile strength) for Soaked condition.

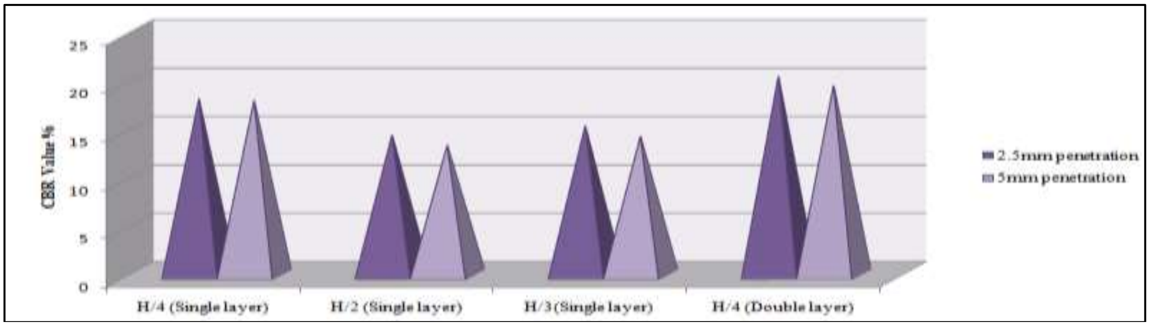

Fig :7.2(b): CBR values with varying position of geogrid reinforcement (20 kN/m tensile strength) for unsoaked condition.

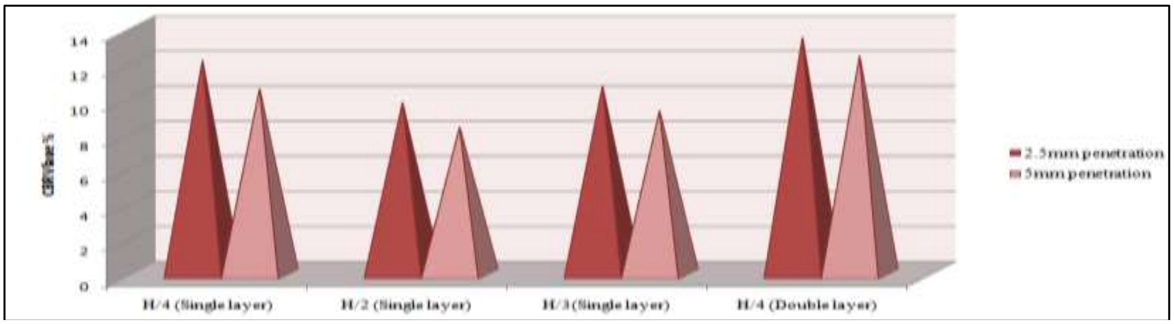

Fig :7.3(a): CBR values with varying position of geogrid reinforcement (4.07 kN/m tensile strength) for Soaked condition.

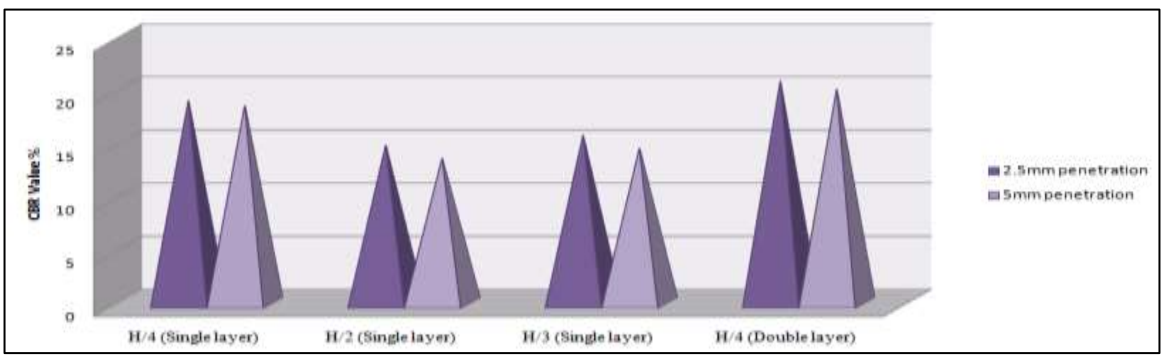

Fig:7.3(b): CBR values with varying position of geogrid reinforcement (4.07kN/m tensile strength) for unsoaked condition.

The improvement in CBR can be attributed to the ability of geogrids to reduce penetration and deformation while promoting more effective stress distribution within the soil. The reinforcement develops mechanical interlocking and frictional interaction with surrounding soil particles, allowing tensile forces to be mobilized that limit lateral soil movement and increase the overall stiffness and strength of the subgrade. This mechanism has been reported by Kamel et al. (2004).

Furthermore, geogrid reinforcement disperses the applied load over a wider area, thereby reducing the vertical stresses transmitted to the underlying weak subgrade. The resulting reduction in stress concentration improves the bearing capacity and overall stability of the reinforced soil system, consistent with the observations of Giroud et al. (1981).

Table 6. CBR values and improvement factors for reinforcement placed at H/4 (10% fly ash).

Configuration	Soaked CBR 2.5 mm (%)	Soaked CBR 5.0 mm (%)	Unsoaked CBR 2.5 mm (%)	Unsoaked CBR 5.0 mm (%)	Improvement factor, soaked 2.5 mm
Red soil (untreated)	1.40	1.20	4.66	4.10	—

Red soil + 10% FA (unreinforced)	9.31	7.40	14.43	16.14	1.00
Red soil + 10% FA + G1 at H/4	12.11	10.86	19.09	18.63	1.30
Red soil + 10% FA + G2 at H/4	11.64	10.64	18.16	18.00	1.25
Red soil + 10% FA + G3 at H/4	12.18	10.55	20.95	18.63	1.31

4.4 Large-scale unconfined compressive strength behaviour

Fourteen large-scale UCS configurations were tested, comprising two unreinforced specimens (untreated red soil and red soil with 10% fly ash) and twelve reinforced specimens obtained by combining three geogrid types with four reinforcement layouts. As noted in Section 3, conventional 38 mm diameter specimens were unsuitable for this programme because the 38 mm aperture of geogrids G1 and G2 equalled the specimen diameter, so that no complete aperture could be enclosed within the soil and no interlock could develop. The 100 mm diameter mould accommodates approximately two and a half apertures across the specimen width for G1 and G2 and approximately twelve for G3, allowing load transfer through the reinforcement to be mobilised. All specimens were compacted at their respective optimum moisture content and maximum dry density, maintained a height-to-diameter ratio of 2:1, and were tested immediately after preparation at a constant axial displacement rate of 0.89 mm/min. Load and deformation were recorded continuously and the peak of the resulting stress–strain curve was taken as the UCS. The results are summarised in Table 4.

The unreinforced stabilised soil reached 300 kPa against 237 kPa for the untreated red soil, an increase of 27% consistent with the CBR trend. All reinforced specimens exceeded the unreinforced stabilised value. Single-layer reinforcement produced moderate gains of 2% to 10% depending on geogrid and depth, whereas double-layer reinforcement at 2×H/4 produced gains of 68% to 88%, the highest value of 565 kPa being recorded for geogrid G3. Relative to the untreated red soil, this represents an increase of 2.4 times.

4.5 Failure Mechanism and Discussion

The UCS results (Table 4) show that all reinforced specimens achieved higher compressive strengths than the corresponding unreinforced soil. The improvement is attributed to the reinforcing action of the geogrid, which distributes applied stresses more effectively and delays the development of failure.During loading, stresses are transferred from the soil to the geogrid through interlocking, friction, and interface adhesion. This interaction mobilizes tensile resistance within the reinforcement, restraining lateral soil deformation and improving the integrity of the soil–geogrid composite. In contrast, unreinforced specimens experience greater stress concentration and larger deformations, resulting in earlier ductile failure. The peak stress obtained from the stress–strain curve was considered the UCS of each specimen.

Table 4. Large-scale UCS test results

Combination		**UCS Unreinforced test results in kPa**	
Red Soil		237	
Red Soil+10% FA		300	
	UCS Reinforced test results in kPa		
Geogrid type	**G1**	**G2**	**G3**
Red Soil+10% FA+ G(H/2)	317	306	321
Red Soil+10%FA+ G(H/3)	319	315	325
Red Soil+10%FA+ G(H/4)	322	324	331
Red Soil+10% FA+G(2*H/4)	539	504	565

A. Effect of Specimen Size

The influence of specimen size was evaluated using both conventional and large-scale UCS specimens prepared with untreated red soil and red soil stabilized with 10% fly ash. All specimens were compacted at their respective optimum moisture content and maximum dry density while maintaining a height-to-diameter ratio of 2:1.

As presented in Table 5, UCS decreased with increasing specimen size. The failure patterns shown in Fig. 8 indicate that larger specimens contained greater material heterogeneity, including pores, microcracks, and other inherent discontinuities, which reduced compressive strength. In contrast, smaller specimens exhibited a more uniform internal structure with fewer defects, resulting in higher UCS values. These observations confirm that specimen size significantly influences the measured compressive strength of both untreated and stabilized soils.

Table 5: UCS values (kPa) of large-scale and small-scale specimens without reinforcement

Combination(UCS Value)	Soil	Soil+10% FA
Small-scale specimen(kPa)	308	387
Large-scale specimen(kPa)	237	300

Fig 8: Failure patterns in large-scale (A) and small-scale (B) UCS specimens stabilized with 10% Fly Ash.

B. Effect of Reinforcement Position, Number of Layers, and Geogrid Type

Table 4 demonstrates that geogrid reinforcement substantially enhances UCS, particularly when combined with 10% fly ash stabilization. The highest strength was obtained when reinforcement was placed at H/4, where tensile membrane action effectively reduced stress concentration while fly ash improved inter particle bonding through soil aggregation.

Failure modes for different reinforcement positions are presented in Figs. 9 and 10. Double-layer reinforcement (2H/4) produced failure surfaces extending from both the upper and lower portions of the specimen, whereas single-layer reinforcement at H/4 localized failure near the reinforcement level. For H/3 and H/4 configurations, failure generally propagated from the lower region toward the centre without reaching the upper portion, indicating that the reinforcement provided additional confinement to the soil above the geogrid.Specimens reinforced at mid-height (H/2) exhibited comparatively irregular failure patterns between the upper and lower halves. This behaviour is likely associated with slight density variations introduced during specimen compaction, producing unequal deformation within the sample, consistent with the observations of Vihan (2020). Overall, reinforcement position strongly influenced both strength and failure behaviour, with H/4 providing the most effective confinement.

Fig. 9. Failure patterns of specimens reinforced at (A) H/2, (B) H/3, and (C) H/4.

Fig. 10. Failure patterns of specimens reinforced at (A) 2H/4 and (B) H/2.

Increasing the number of reinforcement layers further improved UCS. Double-layer reinforcement consistently produced higher strengths than single-layer configurations because the additional geogrid increased internal confinement, distributed stresses more uniformly, and intercepted potential failure planes. Although the difference between H/2 and 2H/4 arrangements was relatively small, the latter showed better resistance to deformation by restraining failure from both ends of the specimen.Among the three geogrids, G3 provided the highest UCS values, reaching 331 kPa for single-layer reinforcement and 565 kPa for double-layer reinforcement. Despite its lower tensile strength, G3 outperformed G1 and G2 because its smaller aperture size (8 mm) promoted stronger soil–geogrid interlocking and greater interface contact. In contrast, the larger 38 mm apertures of G1 and G2 reduced interaction with the surrounding soil. These results indicate that aperture geometry can have a greater influence on reinforcement efficiency than tensile strength alone.

4.6 Improvement factors and implications for subgrade design

Table 7 summarises the improvement factors derived from Tables 3, 4 and 6, expressed relative both to the untreated red soil and to the unreinforced 395tabilizer soil. Presenting the results in this 395tabilizer form separates the contribution of the 395tabilizer from that of the reinforcement and permits direct comparison with values reported elsewhere in the literature.

Table 7. Summary of improvement factors for stabilised and reinforced red soil.

Property	Untreated red soil	10% FA (unreinforced)	10% FA + G3 at H/4	10% FA + G3 at 2×H/4
Soaked CBR, 2.5 mm (%)	1.40	9.31	12.18	see Fig. 7.3(a)
Unsoaked CBR, 2.5 mm (%)	4.66	14.43	20.95	see Fig. 7.3(b)
Large-scale UCS (kPa)	237	300	331	565
UCS improvement over untreated soil	1.00	1.27	1.40	2.38

UCS improvement over stabilised soil	—	1.00	1.10	1.88

Two features of Table 7 deserve comment. First, the contribution of the stabiliser and that of a single geogrid layer are of comparable magnitude in UCS terms, whereas in CBR terms the stabiliser dominates. This is expected: the CBR test loads a small plunger at the specimen surface and is governed largely by the stiffness of the near-surface material, whereas the UCS test loads the full cross-section and therefore registers the tensile membrane action of the reinforcement more directly. Second, the increase associated with the second geogrid layer is disproportionately large relative to the increase produced by the first. Adding one layer at H/4 raises the UCS by approximately 10%, while adding a second layer at the mirrored position raises it by a further 71%. A simple superposition of reinforcement contributions would not predict this.

A plausible explanation is that a single layer at H/4 intercepts only the upper of the two conjugate failure surfaces that form in an unconfined specimen, so that failure simply migrates to the unreinforced lower half; the failure patterns in Figs. 9 and 10 support this reading, since single-layer specimens failed predominantly below the reinforcement. When both conjugate surfaces are intercepted, no continuous failure plane can develop through the specimen and the mode changes from shear on a discrete plane to distributed bulging, which requires a substantially higher axial stress. The strength gain is therefore a consequence of a change in failure mechanism rather than of an incremental increase in reinforcement area.

Two observations support this reading. The failure photographs in Figs. 9 and 10 show that single-layer specimens developed their principal failure surface predominantly below the reinforcement, whereas double-layer specimens developed surfaces in both the upper and lower portions without a single continuous plane traversing the specimen. Further, the ranking of the three geogrids was preserved between the single- and double-layer arrangements, which would not be expected if the double-layer result were an artefact of differential compaction rather than a reinforcement effect. The interpretation nevertheless remains an inference drawn from strength and failure geometry rather than a direct measurement, and Section 4.7 identifies the additional measurements that would confirm it.

From a design standpoint, the practical significance of these results lies in the transition of the subgrade from an unacceptable to a usable classification. Pavement design procedures based on subgrade CBR require the layer thickness above the subgrade to increase sharply as the design CBR falls below approximately 5%, and subgrades with soaked CBR values of the order of 1% to 2% generally require removal and replacement or treatment before a pavement can be founded on them. Raising the soaked CBR of the red soil from 1.40% to 9.31% by the addition of 10% fly ash, and to approximately 12% with a single geogrid layer at H/4, moves the material from the first category to the second and correspondingly reduces the thickness of imported granular material required above it. Where high-quality granular material is unavailable locally or attracts high haulage costs, this reduction is the principal economic justification for the treatment.

The practical significance of these results lies in the change of subgrade classification that they produce. In CBR-based pavement design, the thickness of granular material required above the subgrade increases sharply as the design CBR falls below about 5%, and subgrades with soaked CBR values of the order of 1% to 2% are generally treated as unsuitable, requiring removal and replacement or in-situ treatment before a pavement can be founded on them. Raising the soaked CBR of the red soil from 1.40% to 9.31% by the addition of 10% fly ash, and to approximately 12% with a single geogrid layer at H/4, moves the material out of that category and into a range where it can carry the pavement structure directly. Where good-quality granular material is unavailable locally or attracts high haulage costs, the resulting reduction in imported material is the principal economic justification for the treatment. The corresponding thickness saving is design-specific and depends on the traffic level, the design procedure adopted and the properties of the overlying layers; a worked design comparison for a nominated traffic category is beyond the scope of the present laboratory study and is identified in Section 4.7 as a direction for further work.

4.7 Limitations of the study

Four limitations should be borne in mind when interpreting the results. First, all specimens were tested either immediately after compaction or after a four-day soak, so the results characterise the immediate mechanical improvement and do not capture any long-term pozzolanic strength development that the Class F ash might contribute over weeks or months in the field. Second, the reinforcement was tested under monotonic loading only; pavement subgrades are subjected to repeated loading, and the cyclic response of the reinforced composite — in particular the accumulation of permanent deformation — was not investigated. Third, although the 100 mm mould substantially reduces the boundary constraint compared with the conventional specimen, it does not eliminate it, and the specimen size effect demonstrated in Table 5 shows that absolute strength values remain scale-dependent; the improvement factors reported here are consequently more transferable than the absolute strengths. Fourth, the proposed change of failure mechanism under double-layer reinforcement is inferred from strength and failure geometry; direct confirmation would require measurement of the axial strain at failure for single- and double-layer specimens, which the present instrumentation did not record. Field verification through plate load or falling weight deflectometer testing on a reinforced trial section, together with a worked pavement thickness comparison for a nominated traffic category, is recommended before the findings are applied in design.

5. Artificial neural network modelling

5.1 Rationale and model formulation

The experimental results of Section 4 show that the strength of the reinforced composite depends on four variables — the tensile strength of the geogrid, its aperture size, the depth at which it is placed and the number of layers used — and that the dependence is not additive. The single-layer arrangements differ from the unreinforced stabilised soil by between 2% and 10%, whereas the double-layer arrangements differ by between 68% and 88%; no linear combination of the four variables can reproduce both regimes. A model capable of representing interaction and threshold behaviour is therefore required if the experimental results are to be generalised, and a feed-forward artificial neural network was adopted for this purpose.

Two networks were developed. Network I predicts the large-scale unconfined compressive strength of the stabilised soil from the four reinforcement variables, using the thirteen configurations of Table 4 that share a common fly ash dosage of 10% (one unreinforced control and twelve reinforced arrangements). The inputs are the geogrid tensile strength T (kN/m), the aperture size A (mm), the normalised placement depth d/H and the number of reinforcement layers N; the unreinforced control is encoded as T = A = d/H = N = 0. Network II predicts the soaked CBR at 2.5 mm and 5.0 mm penetration from the fly ash content alone, using the eight mixtures of Table 3, and is used as a continuous surrogate for locating the optimum dosage between the discrete tested values. The two datasets are summarised in Table 8.

Table 8. Datasets used for artificial neural network development.

Network	Target	Inputs	Samples	Input ranges
I	Large-scale UCS (kPa)	T, A, d/H, N	13	T: 0–40 kN/m; A: 0–38 mm; d/H: 0–0.50; N: 0–2
II	Soaked CBR at 2.5 and 5.0 mm (%)	Fly ash content (%)	8	Fly ash: 0–20%

5.2 Network architecture and training

All inputs and targets were scaled to the interval [0, 1] before training. A fully connected feed-forward architecture with hyperbolic tangent activation in the hidden layers and linear output was used, trained by the L-BFGS quasi-Newton algorithm with L2 weight decay. Because the datasets are small, the architecture and the weight-decay coefficient were not fixed a priori but selected by search over hidden-layer configurations of (3), (4), (5), (6) and (4, 3) neurons and weight-decay values of 0.001, 0.01, 0.1 and 1.0. To avoid the optimistic bias that arises when the same data are used both to choose and to evaluate a model, selection was carried out inside an inner leave-one-out loop nested within an outer leave-one-out loop, so that the observation held out for testing took no part in either architecture selection or weight estimation. The configuration selected in twelve of the thirteen outer folds for Network I was two hidden layers of four and three neurons with a weight-decay coefficient of 0.001, giving the 4–4–3–1 architecture shown in Fig. 11. Network II adopted the same hidden-layer configuration with a weight-decay coefficient of 0.01. Because L-BFGS converges to a local optimum that depends on the random initialisation of the weights, all reported predictions are the mean of an ensemble of twenty networks trained from different random seeds; ensembling removes the dependence of the results on any single initialisation.

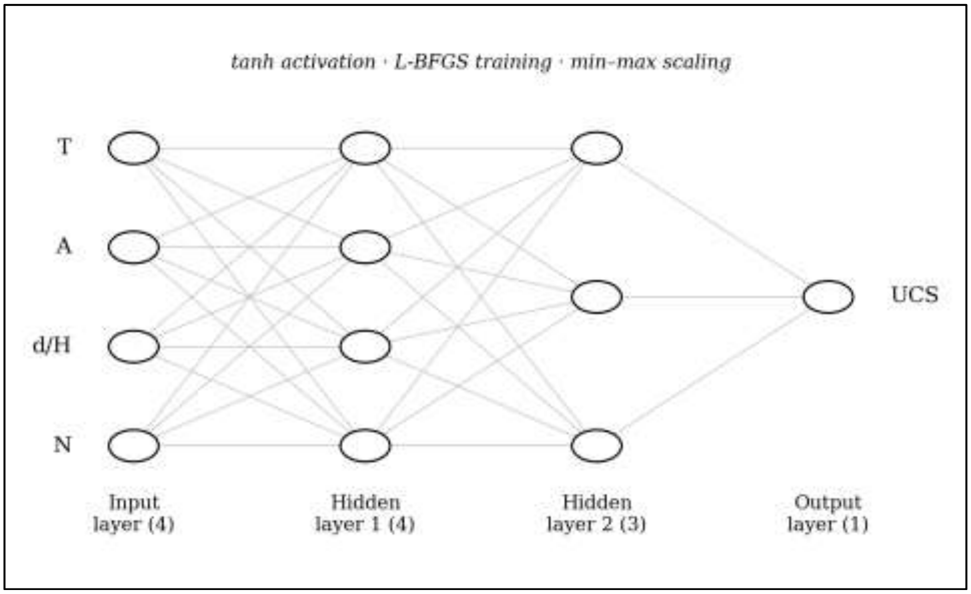

Fig. 11. Architecture of Network I for prediction of large-scale UCS.

5.3 Predictive performance

Table 9 compares the cross-validated performance of the two networks with that of multiple linear regression models trained and validated by the identical procedure. For Network I the artificial neural network achieved a leave-one-out coefficient of determination of 0.969 with a root mean square error of 16.4 kPa and a mean absolute percentage error of 2.3%, against 0.671, 53.3 kPa and 11.1% respectively for multiple linear regression. The error of the network is thus approximately one-third that of the linear model, and is of the same order as the repeatability that would be expected between nominally identical compacted specimens. The parity plots in Fig. 12 show that the linear model systematically over-predicts the single-layer results and under-predicts the double-layer results, which is the signature of a model attempting to fit two distinct response regimes with one gradient; the network reproduces both.

For Network II the network reached leave-one-out coefficients of determination of 0.630 and 0.593 for the soaked CBR at 2.5 mm and 5.0 mm penetration, against negative values for the corresponding linear models. A negative coefficient indicates that the linear model predicts less accurately than the sample mean, which is the expected outcome when a linear function is fitted to a response that rises to a maximum and then falls. The absolute accuracy of Network II is nevertheless modest: with eight observations, the removal of any single point materially alters the shape of the fitted curve, and the network is therefore reported here as an interpolating surrogate rather than as a predictive tool.

Table 9. Cross-validated performance of the neural network and linear regression models.

Model	**Target**	**R^2 (LOOCV)**	**RMSE (LOOCV)**	**MAE (LOOCV)**	**MAPE (%)**
ANN Network I	UCS (kPa)	0.969	16.4 kPa	10.5 kPa	2.3
MLR (same inputs)	UCS (kPa)	0.671	53.3 kPa	37.2 kPa	11.1
ANN Network II	Soaked CBR, 2.5 mm (%)	0.630	1.66%	1.43%	35.0
MLR (same input)	Soaked CBR, 2.5 mm (%)	−0.524	3.36%	3.22%	83.2
ANN Network II	Soaked CBR, 5.0 mm (%)	0.593	1.40%	1.28%	38.7
MLR (same input)	Soaked CBR, 5.0 mm (%)	−0.376	2.57%	2.49%	75.9

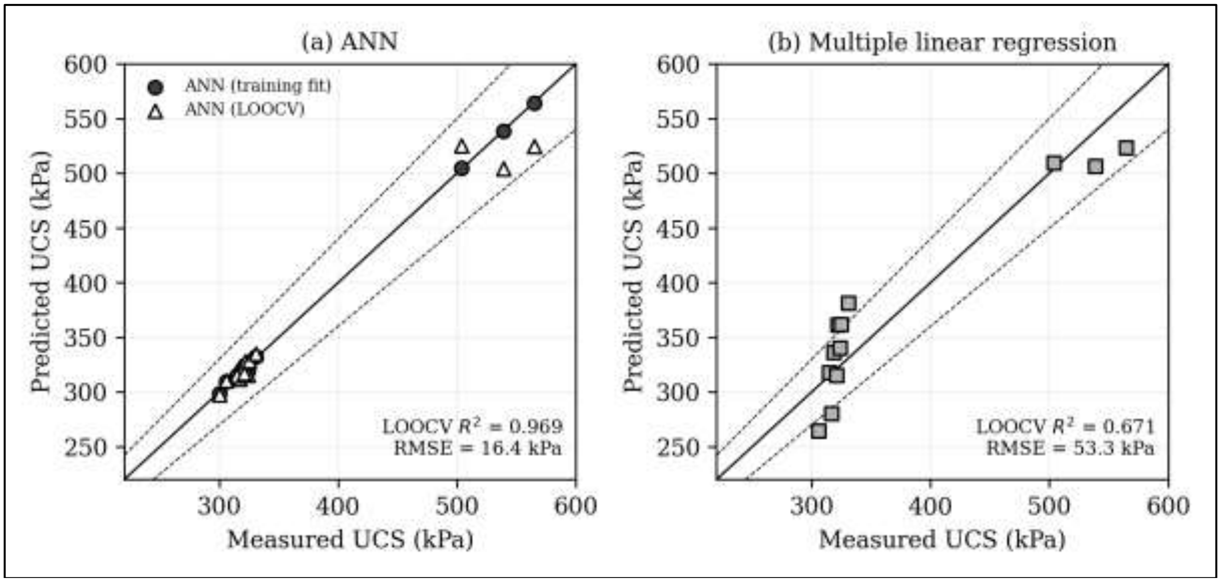

Fig. 12. Predicted against measured large-scale UCS: (a) artificial neural network; (b) multiple linear regression. Dashed lines indicate the ±10% error band.

5.4 Relative importance of the input variables

The trained ensemble of Network I was interrogated to establish the relative contribution of each input. Two independent methods were used: Garson's algorithm, which partitions the products of the absolute connection weights along each input–output path, and permutation importance, which measures the increase in mean square error when the values of one input are randomly permuted across the dataset. The two methods rest on different assumptions — the first is a property of the fitted weights and the second of the model's predictions — so agreement between them is meaningful. The results are shown in Fig. 13.

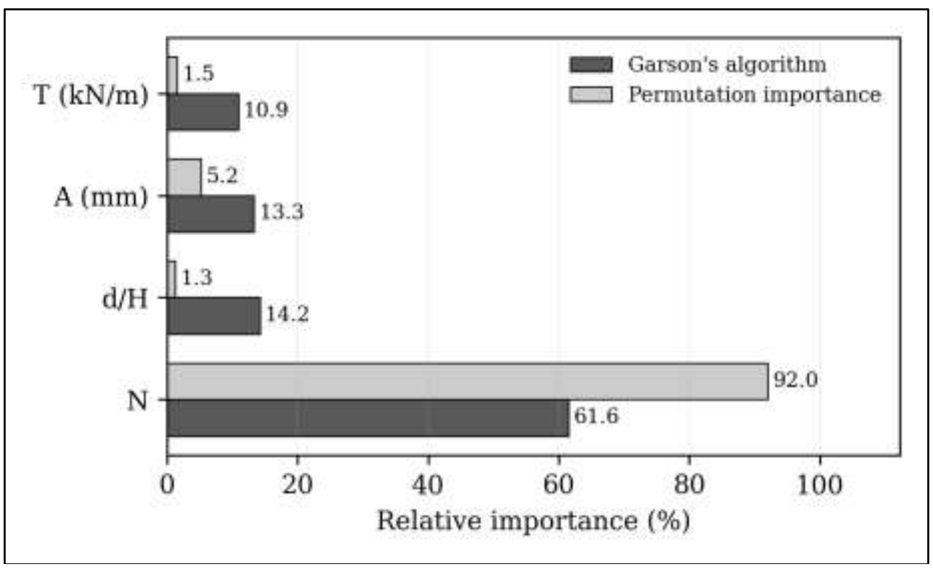

Fig. 13. Relative importance of the input variables of Network I by Garson's algorithm and by permutation importance.

Both methods identify the number of reinforcement layers as the dominant variable, contributing 61.6% by Garson's algorithm and 92.0% by permutation importance. The difference in magnitude between the two figures reflects the difference in what they measure: permutation importance is dominated by the variable that separates the two response regimes, whereas Garson's algorithm distributes influence across all paths in the network. The ordering is the same in both cases and is consistent with the experimental observation that the step from one layer to two produces a far larger change in strength than any variation within the single-layer arrangements.

The result of principal interest concerns the two geogrid product properties. Both methods rank aperture size above tensile strength — 13.3% against 10.9% by Garson's algorithm and 5.2% against 1.5% by permutation importance — with the permutation analysis indicating that tensile strength is the least influential of the four inputs. This is a quantitative statement of the qualitative conclusion drawn in Section 4.5 from the superior performance of geogrid G3, and it carries a direct practical implication. Geogrid specifications for subgrade applications are commonly written in terms of a minimum ultimate tensile strength, a criterion that would have selected G1 or G2 over G3 in this programme and would have produced the poorer outcome. The network indicates that, over the range of products examined, tensile strength has little explanatory power for the strength of a fine-grained stabilised subgrade once the aperture geometry is accounted for. It must be stressed that this conclusion applies within the tested range and to a fine-grained soil: for a coarse granular fill, or at tensile forces approaching the rupture capacity of the reinforcement, tensile strength would necessarily become governing.

5.5 Surrogate optimisation of the fly ash dosage

The experimental programme identified 10% as the optimum fly ash content because that was the highest-performing of the discrete dosages tested. The true optimum, however, need not coincide with a tested value. Network II was therefore evaluated continuously over the interval from 0% to 20% fly ash at increments of 0.05%, and the resulting response curves are shown in Fig. 14. The surrogate places the maximum soaked CBR at 8.9% fly ash for 2.5 mm penetration and at 9.0% for 5.0 mm penetration, in both cases marginally below the tested optimum. The predicted peak values, 9.19% and 7.49%, are slightly lower than the measured values at 10% fly ash, which reflects the smoothing inherent in fitting a continuous function through scattered points and means that the peak magnitude should be read from the measurements rather than from the curve.

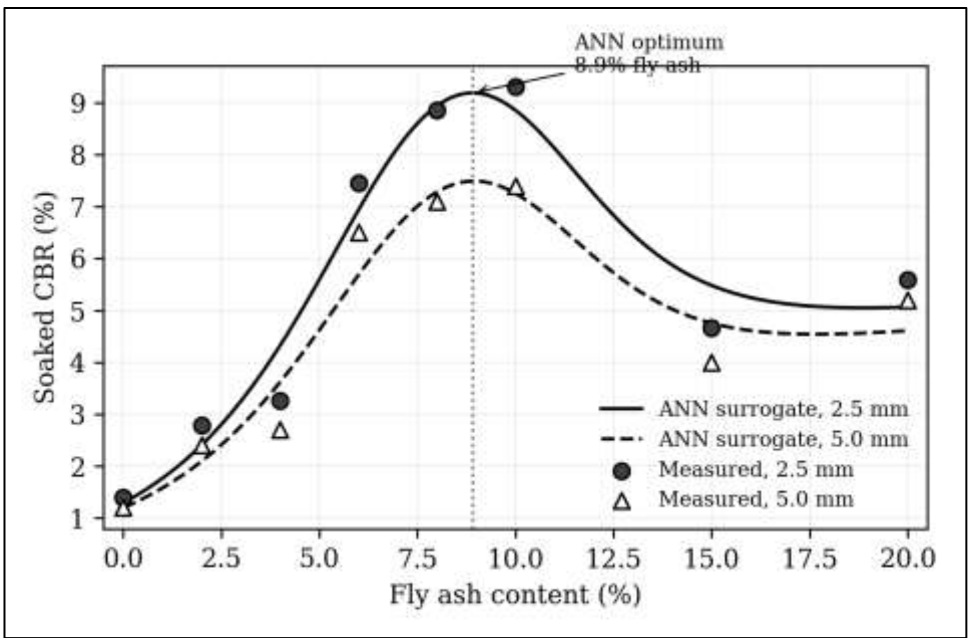

Fig. 14. Network II used as a continuous surrogate for the soaked CBR response, with the measured values superimposed.

The practical conclusion is that the optimum dosage lies between approximately 8% and 10% and that the response in this interval is flat: between 8% and 10% fly ash the predicted soaked CBR at 2.5 mm varies by less than 0.4 percentage points. A dosage specified anywhere in that range would therefore deliver essentially the same performance, and the lower end of the range would do so with a smaller quantity of ash. The curve also shows that the response falls away far more rapidly above the optimum than it rises below it, so that under-dosing is less damaging than over-dosing — a useful margin to have identified where field batching tolerances are wide.

5.6 Scope and limitations of the models

The models presented here are calibrated on thirteen and eight observations respectively and their scope is correspondingly narrow. Three restrictions apply. First, the networks are interpolators and must not be extrapolated: Network I is valid only for tensile strengths from 4.07 to 40 kN/m, apertures from 8 to 38 mm, placement depths from H/4 to H/2 and one or two reinforcement layers, at a fly ash dosage of 10% and for the specific red soil tested, and Network II only for fly ash dosages from 0% to 20% of that same soil. Second, because aperture size and tensile strength are strongly correlated in the three commercial products examined — the two high-strength geogrids share the 38 mm aperture and the low-strength geogrid has the 8 mm aperture — the dataset cannot fully separate the two effects. The finding that aperture outranks tensile strength is therefore best regarded as a testable hypothesis supported by two independent sensitivity measures, and its confirmation requires a factorial programme in which aperture and tensile strength are varied independently. Third, the leave-one-out estimates reported in Table 9 are themselves subject to sampling variability at these sample sizes, and the performance of Network I in particular rests on correctly reproducing four double-layer observations. Enlarging the dataset — by testing additional geogrid products, intermediate placement depths and three-layer arrangements — is the natural next step and would allow both the model and the importance ranking to be tested rather than merely reported.

6. Conclusions

Based on the experimental investigation reported above, the following conclusions are drawn.

- The unconfined compressive strength and the California Bearing Ratio of the red soil both increase with fly ash addition up to a dosage of 10% by dry weight and decline beyond it. A fly ash content of 10% is therefore established as the optimum for the soil investigated, simultaneously on compaction, UCS and CBR criteria.
- At the optimum dosage the soaked CBR at 2.5 mm penetration increased from 1.40% to 9.31% and the unsoaked CBR from 4.66% to 14.43%, corresponding to improvement factors of 6.7 and 3.1 respectively. The large-scale UCS increased from 237 kPa to 300 kPa. Because the ash used is a Class F pozzolan with low free lime and the specimens were tested without curing, these gains are attributed primarily to improved gradation and denser particle packing rather than to cementitious reaction.
- For all three geogrids and under both soaked and unsoaked conditions, a single reinforcement layer placed at H/4 from the loaded face was more effective than placement at H/3 or H/2. Double-layer reinforcement at H/4 from both faces was more effective still, raising the UCS of the stabilised soil from 300 kPa to 565 kPa, an increase of 88%.
- The disproportionate gain associated with the second reinforcement layer is attributed to the interception of both conjugate failure surfaces, which suppresses the formation of a continuous failure plane and changes the failure mode from discrete shear to distributed bulging.
- The geogrid with the lowest tensile strength (4.07 kN/m) gave the highest strength improvement at every position tested, outperforming products rated at 20 kN/m and 40 kN/m. Its 8 mm aperture is compatible with the particle size of the fine-grained stabilised soil, whereas the 38 mm apertures of the stronger geogrids are too coarse to develop effective interlock. For fine-grained subgrades, aperture geometry is therefore a more important selection criterion than rated tensile strength, and specifications written around tensile strength alone may select a less effective product.
- The combined use of 10% Class F fly ash and a small-aperture biaxial geogrid placed at H/4 offers a practical and sustainable route to improving weak red soil subgrades, reducing dependence on imported granular material while providing a beneficial outlet for a bulk industrial by-product.
- An artificial neural network with two hidden layers, validated by nested leave-one-out cross-validation, predicted the large-scale UCS of the reinforced stabilised soil with a coefficient of determination of 0.969 and a root mean square error of 16.4 kPa, against 0.671 and 53.3 kPa for a multiple linear regression using the same inputs. The reinforced response is therefore strongly non-linear, and linear models are not adequate to represent it.
- Sensitivity analysis of the trained network by two independent methods identified the number of reinforcement layers as the dominant variable and ranked aperture size above tensile strength among the geogrid product properties, with tensile strength the least influential of the four inputs by permutation importance. This quantifies the experimental finding and indicates that geogrid specifications for fine-grained subgrades written solely around a minimum tensile strength may select a less effective product.
- A second network, used as a continuous surrogate over the fly ash dosage range, located the soaked CBR optimum at approximately 9% fly ash and showed the response to be flat between 8% and 10% and to fall away more steeply above the optimum than below it, indicating that a dosage specified at the lower end of that range is both adequate and economical.

Acknowledgements
The authors gratefully acknowledge the Department of Civil Engineering, University Visvesvaraya College of Engineering, Bangalore University, for providing the laboratory facilities used in this investigation, and M/s Geotech Industries Pvt Ltd, Gujarat, for supplying the geogrid materials and the associated product specifications.
This research did not receive any specific grant from funding agencies in the public, commercial or not-for-profit sectors.

Declaration of competing interest
The authors declare that they have no known competing financial interests or personal relationships that could have appeared to influence the work reported in this paper.

Data availability
The data supporting the findings of this study are available from the corresponding author on reasonable request.

7. References

[1] AASHTO. (2009). Standard practice for geosynthetic reinforcement of the aggregate base course of flexible pavement structures. Washington, D.C.: American Association of State Highway and Transportation Officials.
[2] Abd El Halim, A., Haas, R., and Chang, W. (1983). Geogrid reinforcement of asphalt pavements and verification of elastic layer theory. Transportation Research Record, (949), 55–65.
[3] Baskar, K., Keerthana, K., Sakthisri, R., and Sona, R. (2022). Effect of calcium carbide residue and fly ash in soil stabilization for sand mixed clayey soil. Materials Today: Proceedings, 69(3), 1253–1259. https://doi.org/10.1016/j.matpr.2022.08.323
[4] Choudhary, A. K., Gill, K. S., Jha, J. N., and Shukla, S. K. (2012). Improvement in CBR of the expansive soil subgrades with a single reinforcement layer. Proceedings of the Indian Geotechnical Conference, 289–292.
[5] Takhelmayum, G., Savitha, A. L., and Gudi, K. (2013). Laboratory study on soil stabilization using fly ash mixtures. International Journal of Engineering Science and Innovative Technology, 2(1), 477–482.
[6] Duncan-Williams, E., and Attoh-Okine, N. O. (2008). Effect of geogrid in granular base strength — An experimental investigation. Construction and Building Materials, 22(11), 2180–2184. https://doi.org/10.1016/j.conbuildmat.2007.08.008
[7] Fannin, R. J., and Sigurdsson, O. (1996). Field observations on stabilization of unpaved roads with geosynthetics. Journal of Geotechnical Engineering, 122(7), 544–553. https://doi.org/10.1061/(ASCE)0733-9410(1996)122:7(544)
[8] Giroud, J. P., and Noiray, L. (1981). Geotextile-reinforced unpaved road design. Journal of the Geotechnical Engineering Division, 107(9), 1233–1254.
[9] Kamel, M. A., Chandra, S., and Kumar, P. (2004). Behaviour of subgrade soil reinforced with geogrid. International Journal of Pavement Engineering, 5(4), 201–209. https://doi.org/10.1080/10298430412000327122
[10] Calvarano, L. S., and Palamara, R. (2016). Unpaved road reinforced with geosynthetics. Procedia Engineering, 158, 296–301.
[11] Singh, M., Trivedi, A., and Shukla, S. K. (2019). Strength enhancement of the subgrade soil of unpaved road with geosynthetic reinforcement layers. Transportation Geotechnics, 19, 54–60. https://doi.org/10.1016/j.trgeo.2019.01.007
[12] Ozdemir, M. A. (2016). Improvement in bearing capacity of a soft soil by addition of fly ash. Procedia Engineering, 143, 498–505. https://doi.org/10.1016/j.proeng.2016.06.063
[13] Nawaz, I. (2013). Disposal and utilization of fly ash to protect the environment. International Journal of Innovative Research in Science, Engineering and Technology, 2(10), 5259–5266.
[14] Rai, P., and Qiu, W. (2021). Effect of fly ash and cement on the engineering characteristic of stabilized subgrade soil. Advances in Civil Engineering, 2021, Article 1368194. https://doi.org/10.1155/2021/1368194
[15] Rajesh, U., Sajja, S., and Chakravarthi, V. K. (2016). Studies on engineering performance of geogrid reinforced soft subgrade. Transportation Research Procedia, 17, 164–173.

[16] Deshmukh, R. R., Patel, S., and Shahu, J. T. (2021). Field assessment of improvement in composite modulus of geosynthetic-reinforced pavements. Geosynthetics International, 28(4), 1–14.
[17] Jayawardane, V. S., and Anggraini, V. (2020). Strength enhancement of geotextile-reinforced fly ash-based geopolymer stabilized residual soil. International Journal of Geosynthetics and Ground Engineering, 6, Article 50, 2–15.
[18] ASTM C618-03. (2003). Standard specification for coal fly ash and raw or calcined natural pozzolan for use in concrete. West Conshohocken, PA: ASTM International.
[19] IS 2720 (Part 7). (1980). Methods of test for soils — Determination of water content–dry density relation using light compaction. New Delhi: Bureau of Indian Standards.
[20] IS 2720 (Part 10). (1991). Methods of test for soils — Determination of unconfined compressive strength. New Delhi: Bureau of Indian Standards.
[21] IS 2720 (Part 16). (1987). Methods of test for soils — Laboratory determination of CBR. New Delhi: Bureau of Indian Standards.
[22] Shahin, M. A., Jaksa, M. B., and Maier, H. R. (2001). Artificial neural network applications in geotechnical engineering. Australian Geomechanics, 36(1), 49–62.
[23] Shahin, M. A., Jaksa, M. B., and Maier, H. R. (2009). Recent advances and future challenges for artificial neural systems in geotechnical engineering applications. Advances in Artificial Neural Systems, 2009, Article 308239. https://doi.org/10.1155/2009/308239
[24] Taskiran, T. (2010). Prediction of California bearing ratio (CBR) of fine grained soils by AI methods. Advances in Engineering Software, 41(6), 886–892.
https://doi.org/10.1016/j.advengsoft.2010.01.003
[25] Das, S. K., Samui, P., and Sabat, A. K. (2011). Application of artificial intelligence to maximum dry density and unconfined compressive strength of cement stabilized soil. Geotechnical and Geological Engineering, 29(3), 329–342. https://doi.org/10.1007/s10706-010-9379-4
[26] Garson, G. D. (1991). Interpreting neural network connection weights. AI Expert, 6(4), 46–51.
[27] Breiman, L. (2001). Random forests. Machine Learning, 45(1), 5–32.
https://doi.org/10.1023/A:1010933404324